

Preferred Design of Hierarchical Distribution Matching

Tsuyoshi Yoshida, *Member, IEEE*, Magnus Karlsson, *Fellow, OSA; Senior Member, IEEE*, and Erik Agrell, *Fellow, IEEE*

Abstract—Distribution matching and dematching (DM/invDM) are key functions in probabilistic shaping (PS). Recently techniques for low complexity implementation of DM/invDM have been well studied. Our previously proposed hierarchical DM (HiDM) is one of the good candidates, with capacity-approaching performance with reasonable hardware resources. Though we explained the recipe of HiDM construction with a small example having a short DM word length, there might still be difficulties to expand it to longer DM word lengths. To improve the reproducibility of our work, this paper explains the key parameters in an HiDM having a DM word length more than 100 symbols.

Index Terms—Distribution matching, implementation, modulation, optical fiber communication, probabilistic shaping, reverse concatenation.

I. INTRODUCTION

Constellation shaping has been deeply investigated over several decades to approach the Shannon capacity over the Gaussian channel. There are two shaping schemes, geometric shaping [1] and probabilistic shaping (PS) [2], [3]. Coded modulation techniques have received much interest in the optical fiber communication field [5] after the deployment of coherent detection with digital signal processing [4]. Probabilistic amplitude shaping (PAS) [7] proposed in the communication theory field significantly improve the implementation possibility of PS by using reverse concatenation [8]–[10], which means forward error correction (FEC) inside the shaping DM/invDM. The PAS scheme was early examined in optical fiber communications [11] and gave a significant impact in the community.

Fiber-optical communication channels with optical amplifiers are suitable target applications of PS. The first reason is the existence of the linear optical amplifier. When we shape the optical signal, we reduce the average optical power inside an optical modulator, but the power will soon be recovered by optical amplifiers, which gives an almost linear gain without

T. Yoshida visited the Dept. of Microtechnology and Nanoscience, Chalmers University of Technology, SE-412 96 Göteborg, Sweden, and is now with Information Technology R&D Center, Mitsubishi Electric Corporation, Kamakura, 247-8501, Japan. He also belongs to Graduate School of Engineering, Osaka University, Suita, 505-0871, Japan (e-mail: Yoshida.Tsuyoshi@ah.MitsubishiElectric.co.jp).

M. Karlsson is with the Dept. of Microtechnology and Nanoscience and E. Agrell is with the Dept. of Electrical Engineering, both at Chalmers University of Technology.

Patent application of hierarchical distribution matching has done on Aug. 7, 2018 (application number: PCT/JP2018/029578).

This work was partly supported by “Massively Parallel and Sliced Optical Network (MAPLE),” the Commissioned Research of National Institute of Information and Communications Technology (NICT), Japan.

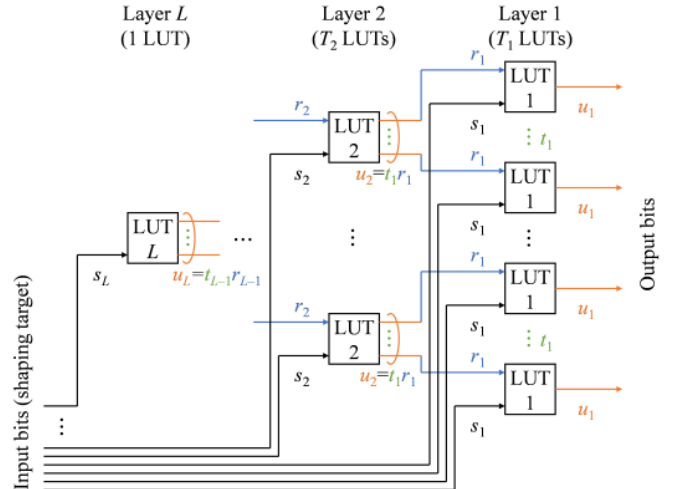


Fig. 1. Schematic of hierarchical DM.

waveform degradation. The second reason is the channel stability because of the confined waveguide (fiber) transmission. Though some signal interferences would remain, a fiber-optical communication channel can be approximated by a Gaussian channel with an average power constraint.

The shaping encoding and decoding functions for PS are called distribution matching (DM) and distribution dematching (invDM), resp. Their high performance and low complexity implementation is one of the hot topics in this field [12]–[31]. Among the DMs, our previously proposed *hierarchical DM (HiDM)* having a unique tree structure of look-up tables (LUTs) shows good performance, reasonable complexity leading to small power consumption for the implementation, high throughput, and small error rate increase in the invDM processing. The paper [27] explained the recipes to configure the LUT tree and to choose the LUT contents for the HiDM by using a small example. However, it would be informative and help others reproduce our results to explain detailed parameters also in the case of long DM word lengths. Thus this paper discloses a set of exemplified LUT interface parameters to design a HiDM having more than 100 quadrature amplitude modulated (QAM) symbols.

II. DESIGN AND EVALUATION OF HIERARCHICAL DM (HiDM)

Fig. 1 shows the schematic of the HiDM [27]. For simplicity, we exclude non-shaped bits from the figure. The parameters in reverse concatenation PS and HiDM are shown

TABLE I
PARAMETERS IN REVERSE CONCATENATION PS SYSTEMS.

| Notation | Description |
|-----------------|--|
| m | number of bits per QAM symbol |
| m^{sb} | number of shaped bits per QAM symbol |
| N_s | number of PAM symbols per DM word |
| N_{in} | number of information bits per DM word |

TABLE II
KEY PARAMETERS IN HIERARCHICAL DM.

| Notation | Description |
|----------|--|
| ℓ | layer index |
| L | number of layers |
| t_ℓ | number of LUTs in layer ℓ connected to an LUT in layer $\ell + 1$ |
| T_ℓ | number of LUTs in layer ℓ |
| r_ℓ | number of input bits in an LUT in layer ℓ from layer $\ell + 1$ |
| s_ℓ | number of input bits in an LUT in layer ℓ as information bits |
| v_ℓ | number of input bits in an LUT in layer ℓ ($r_\ell + s_\ell$) |
| u_ℓ | number of output bits in an LUT in layer ℓ ($mN_s/2$ if $\ell = 1$ or $2r_{\ell-1}$ else) |

in Tabs. I and II, resp. There are N_{in} input bits as a shaping target. They are separately input to LUTs, hierarchically placed in L layers. In the top layer, an LUT receives s_L bits and outputs $u_L = t_{L-1}r_{L-1}$ bits. The r_{L-1} bits are input to an LUT in layer $L - 1$, and the t_{L-1} LUTs in layer $L - 1$ are connected to an LUT in layer L . In layer ℓ ($\neq L$ or 1), each LUT receives r_ℓ bits from layer $\ell + 1$ and s_ℓ bits from the input of the DM as information bits. Totally $v_\ell = r_\ell + s_\ell$ bits are converted into $u_\ell = t_{\ell-1}r_{\ell-1}$ bits, which are fed to layer $\ell - 1$. The number of LUTs in layer ℓ is denoted as T_ℓ . In layer 1 each LUT receives r_1 bits from layer 2 and s_1 bits from the input of the DM. Totally $v_1 = r_1 + s_1$ bits are converted into u_1 bits, which corresponds to u_1/m^{sb} QAM symbols. The number of DM output bits and QAM symbols are $m^{\text{sb}}N_s = T_1u_1 = \prod_{\ell=1}^{L-1} t_\ell u_1$ and $N_s/2$, resp.

In an example for PS-256-QAM generation [27], the total number of bits per complex symbol m is 8, and both the sign bits (the most significant bits) and the least significant bits are not shaped. Only the second and third significant bits are shaped in each dimension, so that $m^{\text{sb}} = 4$. Tab. III exemplifies the parameters used. The number of DM input bits per DM word $\sum_{\ell=1}^L T_\ell s_\ell$ is 507, and the number of DM output bits per DM word $m^{\text{sb}}N_s = T_1u_1$ is 640. Thus the maximum spectral efficiency per 2D symbol at an FEC code rate of 1 is $\beta = 2(2+507/320)$ bit per channel use (bpcu). The entropy of a 2D symbol $2H(X)$ will be larger than β , where X denotes a pulse amplitude modulation (PAM) symbol.

The values of T_ℓ , v_ℓ , and u_ℓ determine the accumulated size of the LUTs, i.e., $\sum_{\ell=1}^L T_\ell 2^{v_\ell} u_\ell$ for DM. When we employ a simple mirror structure for the invDM, its size will be¹ $\sum_{\ell=1}^L T_\ell 2^{u_\ell} v_\ell$. Thus, practically we would have constraints on the values of v_ℓ and u_ℓ , which depend on what hardware resource use is acceptable. Under such a constraint, a binary tree structure $t_\ell = 2$ gives the best shaping performance.

¹Potentially there would be techniques to reduce the LUT size under the same performance.

TABLE III
CHOSEN PARAMETERS USED IN [27, TAB. IV, FIG. 4].

| ℓ | t_ℓ | T_ℓ | r_ℓ | s_ℓ | v_ℓ | u_ℓ |
|--------|----------|----------|----------|----------|----------|----------|
| 7 | 1 | 1 | 5 | 5 | 12 | |
| 6 | 2 | 2 | 6 | 5 | 11 | 12 |
| 5 | 2 | 4 | 6 | 5 | 11 | 12 |
| 4 | 2 | 8 | 6 | 5 | 11 | 12 |
| 3 | 2 | 16 | 6 | 5 | 11 | 12 |
| 2 | 2 | 32 | 6 | 5 | 11 | 12 |
| 1 | 2 | 64 | 6 | 3 | 9 | 10 |

TABLE IV
STATISTICS OF THE SHAPED SIGNALS [27].

| | CCDM | HiDM | MB |
|-----------------------------|--------|--------|--------|
| N_s (PAM symbol) | 320 | 320 | – |
| $P_{ X }(1)$ | 0.2453 | 0.2376 | 0.2628 |
| $P_{ X }(3)$ | 0.2453 | 0.2376 | 0.2355 |
| $P_{ X }(5)$ | 0.1625 | 0.1684 | 0.1891 |
| $P_{ X }(7)$ | 0.1625 | 0.1684 | 0.1360 |
| $P_{ X }(9)$ | 0.0719 | 0.0757 | 0.0877 |
| $P_{ X }(11)$ | 0.0719 | 0.0757 | 0.0506 |
| $P_{ X }(13)$ | 0.0203 | 0.0183 | 0.0262 |
| $P_{ X }(15)$ | 0.0203 | 0.0183 | 0.0121 |
| E | 74.00 | 74.70 | 68.31 |
| $2H(X)$ (bpcu) | 7.242 | 7.252 | 7.169 |
| β at $R_c = 1$ (bpcu) | 7.169 | 7.169 | 7.169 |
| R_{loss} (bpcu) | 0.073 | 0.083 | 0 |
| G (dB) | 1.097 | 1.056 | 1.444 |

We generated PS-256-QAM signals having a DM word length of 320 16-PAM symbols by employing constant composition DM (CCDM) [13] and HiDM [27]. In Tab. IV [27], we summarize the statistics, i.e., the probability mass function P_X , average QAM symbol energy E , QAM symbol entropy $2H(X)$, maximum spectral efficiency β , rate loss $R_{\text{loss}} = 2H(X) - \beta$, and constellation gain $G = (2^\beta - 1)d_{\text{min}}^2/(6E)$, where d_{min} denotes minimum Euclidean distance, of the generated signals. The rate loss of a QAM symbol were 0.07 and 0.08 bpcu for CCDM and HiDM, resp. In each case, the constellation gain was more than 1 dB, whose gap from the ideal Maxwell–Boltzmann (MB) distribution was within 0.4 dB even though we did not shape the least significant bit.

III. SUMMARY

In this contribution we explained the design of HiDM to improve reproducibility also in the case of long symbol sequences. The 7-layer configuration realizes a DM word length of 160 256-QAM symbols. The resulting energy gap from the ideal Maxwell–Boltzmann distribution is less than 0.4 dB, while keeping four bits per QAM symbol uniformly distributed (non-shaped). As shown in [30], this hierarchical DM is useful also for joint source–channel coding. This realizes simultaneous data compression and probabilistic shaping, which can further reduce the required signal-to-noise ratio or system power consumption in future optical networks.

ACKNOWLEDGMENTS

We thank Koji Igarashi of Osaka University for fruitful discussions.

REFERENCES

- [1] G. D. Forney, Jr. and L.-F. Wei, "Multidimensional constellations—Part I: introduction, figure of merit, and generalized cross constellation," *IEEE J. Selected Areas Commun.*, vol. 7, no. 6, pp. 877–892, Aug. 1989.
- [2] A. R. Calderbank and L. H. Ozarow, "Nonequiprobable signaling on the Gaussian channel," *IEEE Trans. Inf. Theory*, vol. 36, no. 4, pp. 726–740, July 1990.
- [3] F. R. Kschischang and S. Pasupathy, "Optimal nonuniform signaling for Gaussian channels," *IEEE Trans. Inf. Theory*, vol. 39, no. 3, pp. 913–929, May 1993.
- [4] K. Roberts, M. O'Sullivan, K.-T. Wu, H. Sun, A. Awadalla, D. J. Krause, and C. Laperle, "Performance of dual-polarization QPSK for optical transport systems," *J. Lightw. Technol.*, vol. 27, no. 16, pp. 3546–3559, Aug. 2009.
- [5] E. Agrell and M. Karlsson, "Power-efficient modulation formats in coherent transmission systems," *J. Lightw. Technol.*, vol. 27, no. 22, pp. 5115–5126, Nov. 2009.
- [6] D. S. Millar, T. Koike-Akino, S. Ö. Arık, K. Kojima, K. Parsons, T. Yoshida, and T. Sugihara, "High-dimensional modulation for coherent optical communications systems," *Opt. Exp.*, vol. 22, no. 7, pp. 8798–8812, Apr. 2014.
- [7] G. Böcherer, F. Steiner, and P. Schulte, "Bandwidth efficient and rate-matched low-density parity-check coded modulation," *IEEE Trans. Commun.*, vol. 63, no. 12, pp. 4651–4665, Dec. 2015.
- [8] W. G. Bliss, "Circuitry for performing error correction calculations on baseband encoded data to eliminate error propagation," *IBM Techn. Disc. Bul.*, vol. 23, pp. 4633–4634, 1981.
- [9] J. L. Fan and J. M. Cioffi, "Constrained coding techniques for soft iterative decoders," in *Proc. Global Telecommunications Conference (GLOBECOM)*, Rio de Janeiro, Brazil, Dec. 1999, vol. 1(B), pp. 723–727.
- [10] I. B. Djordjevic and B. V. Vasic, "Constrained coding techniques for the suppression of intrachannel nonlinear effects in high-speed optical transmission," *J. Lightw. Technol.*, vol. 24, no. 1, pp. 411–419, Jan. 2006.
- [11] F. Buchali, F. Steiner, G. Böcherer, L. Schmalen, P. Schulte, and W. Idler, "Rate adaptation and reach increase by probabilistically shaped 64-QAM: an experimental demonstration," *J. Lightw. Technol.*, vol. 34, no. 7, pp. 1599–1609, Apr. 2016.
- [12] T. V. Ramabadran, "A coding scheme for m -out-of- n codes," *IEEE Trans. Commun.*, vol. 38, no. 8, pp. 1156–1163, Aug. 1990.
- [13] P. Schulte and G. Böcherer, "Constant composition distribution matching," *IEEE Trans. Inf. Theory*, vol. 62, no. 1, pp. 430–434, Jan. 2016.
- [14] J. Cho, S. Chandrasekhar, R. Dar, and P. J. Winzer, "Low-complexity shaping for enhanced nonlinearity tolerance," in *Proc. Eur. Conf. on Opt. Comm. (ECOC)*, Düsseldorf, Germany, Sep. 2016, p. W1C.2.
- [15] G. Böcherer, F. Steiner, and P. Schulte, "High throughput probabilistic shaping with product distribution matching," [Online]. Available: www.arxiv.org/abs/1702.07510
- [16] T. Yoshida, M. Karlsson, and E. Agrell, "Short-block-length shaping by simple mark ratio controllers for granular and wide-range spectral efficiencies," in *Proc. Eur. Conf. on Opt. Comm. (ECOC)*, Göteborg, Sweden, Sep. 2017, p. Tu.2.D.2.
- [17] G. Böcherer, F. Steiner, and P. Schulte, "Fast probabilistic shaping implementation for long-haul fiber-optic communication systems," in *Proc. Eur. Conf. on Opt. Comm. (ECOC)*, Göteborg, Sweden, Sep. 2017, p. Tu.2.D.3.
- [18] M. Pikuš and W. Xu, "Bit-level probabilistically shaped coded modulation," *IEEE Commun. Lett.*, vol. 21, no. 9, pp. 1929–1932, Sep. 2017.
- [19] Y. C. Gültekin, F. M. J. Willems, W. J. Houtum, S. Şerbetli, "Constellation shaping for IEEE 802.11," in *Proc. IEEE 28th Annual Int. Symp. on Personal, Indoor, and Mobile Radio Communications (PIMRC)*, Montreal, Canada, Oct. 2017.
- [20] T. Yoshida, M. Karlsson, and E. Agrell, "Low-complexity variable-length output distribution matching with periodical distribution uniformization," in *Proc. Opt. Fib. Commun. Conf. (OFC)*, San Diego, CA, USA, Mar. 2018, p. M.4.E.2.
- [21] F. Steiner, P. Schulte, and G. Böcherer, "Approaching waterfilling capacity of parallel channels by higher order modulation and probabilistic amplitude shaping," in *Proc. 52nd Annual Conference on Information Sciences and Systems (CISS)*, Princeton, NJ, USA, Mar. 2018.
- [22] Y. C. Gültekin, W. van Houtum, and F. Willems, "On constellation shaping for short block lengths," in *Proc. Symp. on Inf. Theory and Signal Process in the Benelux (SITB)*, Jun. 2018.
- [23] Y. C. Gültekin, F. M. J. Willems, W. J. Houtum, S. Şerbetli, "Approximate enumerative sphere shaping," in *Proc. IEEE Int. Symp. Inf. Theory*, Vail, CO, USA, Jun. 2018, pp. 676–680.
- [24] P. Schulte and F. Steiner, "Divergence-optimal fixed-to-fixed length distribution matching with shell mapping," [Online]. Available: www.arxiv.org/abs/1803.03614
- [25] T. Yoshida, M. Karlsson, and E. Agrell, "Technologies toward implementation of probabilistic constellation shaping," in *Proc. Eur. Conf. on Opt. Comm. (ECOC)*, Roma, Italy, Sep. 2018, p. Th.1.H.1.
- [26] T. Fehenberger, D. S. Millar, T. Koike-Akino, K. Kojima, and K. Parsons, "Multiset-partition distribution matching," *IEEE Trans. Commun.*, vol. 67, no. 3, pp. 1885–1893, Mar. 2019.
- [27] T. Yoshida, M. Karlsson, and E. Agrell, "Hierarchical distribution matching for probabilistically shaped coded modulation," *J. Lightw. Technol.*, vol. 37, no. 6, pp. 1579–1589, Mar. 2019.
- [28] J. Cho, "Prefix-free code distribution matching for probabilistic constellation shaping," [Online]. Available: www.arxiv.org/abs/1810.02411
- [29] Y. Koganei, K. Sugitani, H. Nakashima, and T. Hoshida, "Optimum bit-level distribution matching with at most $O(N^3)$ implementation complexity," in *Proc. Opt. Fib. Commun. Conf. (OFC)*, San Diego, CA, USA, Mar. 2019, Paper M4B.4.
- [30] T. Yoshida, M. Karlsson, and E. Agrell, "Joint source-channel coding via compressed distribution matching in fiber-optic communications," in *Proc. Opt. Fib. Commun. Conf. (OFC)*, San Diego, CA, USA, Mar. 2019, Paper M4B.6.
- [31] J. Cho and P. J. Winzer, "Multi-rate prefix-free code distribution matching," in *Proc. Opt. Fib. Commun. Conf. (OFC)*, San Diego, CA, USA, Mar. 2019, Paper M4B.7.
- [32] European Telecommunications Standards Institute, "Second generation framing structure, channel coding and modulation systems for broadcasting, interactive services, news gathering and other broadband satellite applications; Part 1 (DVB-S2)," ETSI Standard EN 302 307-1 V1.4.1, Nov. 2014. [Online]. Available: www.dvb.org/standards